New Materials, Compounds and Applications
Vol.8, No.3, 2024, pp.411-421
https://doi.org/10.62476/nmca83411

X-RAY DIFFRACTION ANALYSIS, OPTICAL CHARACTERISTICS AND ELECTRO-PHYSICAL PROPERTIES OF THE N-ZnO/P-NiO STRUCTURE GROWN BY THE SPRAY PYROLYSIS METHOD

S.Z. Zainabidinov[1], A.Y. Boboev[1,2], M.B. Rasulova[3], N.Y. Yunusaliyev[1*]

[1]Andijan State University named after Z.M. Bobur, Andijan, Uzbekistan
[2]Institute of Semiconductor Physics and Microelectronics, National University of Uzbekistan, Tashkent, Uzbekistan
[3]Andijan Machine Building Institute, Andijan, Uzbekistan

Abstract. This paper presents X-ray diffraction studies, optical and electrophysical properties of n-ZnO/p-NiO structures. The analysis showed that the ZnO film surfaces exhibit a hexagonal crystal structure, characterized by lattice parameters a = b = 0.3265 nm and c = 0.5212 nm. The deposited NiO films belong to the spatial group Fm3m with lattice parameters of 0.4178 nm. It has been found that the sizes of the subcrystallites of the NiO films were 22.3 nm, 29.3 nm and 16.9 nm, respectively. The grown ZnO and NiO films have a high transmittance coefficient from 74% to 92% and from 56% to 68% in the visible and near-infrared regions of the spectrum, respectively. The optical bandgaps were calculated as 3.27 eV for ZnO, 3.81 eV for NiO and 3.26 eV for the combined ZnO/NiO structure. The volt-ampere characteristics and capacitance-voltage analysis indicate that the n-ZnO/p-NiO structure forms regions with high specific resistances at the heterojunction, with potential for applications in LEDs, solar cells and sensors due to its favorable optical and electrical properties.

Keywords: *Spray-pyrolysis, structure, metal-oxide film, crystalline lattice, subcrystallite.*

Corresponding Author: *N.Y. Yunusaliyev, Andijan State University named after Z.M. Babur, Andijan, Uzbekistan, Tel.: +98948214841; e-mail: nyunusaliyev1997@gmail.com*

Received: *21July 2024;* ***Accepted:*** *28 October 2024;* ***Published:*** *10 December 2024.*

1. Introduction

The development of advanced semiconductor materials has led to significant advancements in optoelectronic and electronic devices, with particular focus on thin-film structures (Mansurov *et al*., 2024). Among these, zinc oxide (ZnO) and nickel oxide (NiO) films have emerged as essential components, owing to their unique combination of structural, optical and electrical properties (Jlassi *et al.*, 2014; Zainabidinov *et al*., 2024a). ZnO, a wide-bandgap n-type semiconductor (Di Mauro *et al*., 2016) and NiO, a p-type semiconductor with high chemical stability (Xia *et al*., 2015), formed a promising heterostructure when combined in the n-ZnO/p-NiO configuration. The study of these heterostructures is of growing interest because of their potential to enhance the performance of a wide range of applications, including light-emitting diodes (LEDs)

How to cite (APA):
Zainabidinov, S.Z., Boboev, A.Y., Rasulova, M.B. & Yunusaliyev, N.Y. (2024). X-ray diffraction analysis, optical characteristics and electro-physical properties of the n-ZnO/p-NiO structure grown by the spray pyrolysis method. *New Materials, Compounds and Applications*, *8*(3), 411-421 https://doi.org/10.62476/nmca83411

(Ohta *et al*., 2003), solar cells, transparent electronics (Xu *et al*., 2020), gas sensors (Ilin *et al*., 2017) and catalysts.

The electrophysical properties of the n-ZnO/p-NiO structure are particularly important for determining its viability in these applications (Martyshov *et al.,* 2014). Parameters such as the electrical conductivity, charge carrier mobility and current transport mechanisms directly affect the efficiency and functionality of the devices. In particular, the n-ZnO/p-NiO heterojunction exhibits a tunnel-recombination mechanism for current conduction, which is crucial for achieving efficient charge separation in photovoltaic cells and enhancing the recombination of electrons and holes in LEDs.

The construction of ZnO/NiO thin films using spray pyrolysis provides a low-cost, scalable method for producing high-quality films with precise control over their thickness and composition (Zainabidinov *et al*., 2024b). Meanwhile, NiO films with a cubic crystal structure (Fm3m space group) and lattice parameters of 0.4178 nm provide p-type conductivity, making them suitable for forming a stable and efficient heterojunction with ZnO. The crystallographic properties of these films play a significant role in their optical and electrical behaviors. For example, the small size of NiO subcrystallites influences their surface area, which can enhance their catalytic activity and sensitivity in gas sensing applications (Tian *et al*., 2016). The crystallographic arrangement of atoms in the ZnO and NiO films directly affects their band structure, which in turn influences their optical absorption and emission behavior. This relationship between the structure and optical properties is critical for optimizing devices such as LEDs, where maximizing light output is essential or in solar cells, where efficient light absorption is key to improving the energy conversion efficiency (Xi *et al*., 2008; Geleta *et al*., 2021).

This study focused on the X-ray diffraction, optical and electrophysical properties of n-ZnO/p-NiO heterostructures grown using the spray pyrolysis method. By analyzing the crystallographic parameters, optical transmittance and electrical conductivity, we aim to provide a deeper understanding of the mechanisms governing the performance of these films in transparent applications. The relevance of this research lies in its potential to contribute to the ongoing development of high-performance low-cost materials for next-generation optoelectronic and electronic devices.

2. Materials and Methods

The deposition of metal oxide films of ZnO and NiO by spray pyrolysis (Zainabidinov *et al*., 2021a) was carried out on a borosilicate glass substrate measuring 10x10x0.170 mm. The surface temperature was measured using a HoldPcakhp-1500 pyrometer. Various temperatures ranging from 300°C to 500°C were tested and the optimal temperatures for ZnO and NiO were 420°C and 340°C, respectively. These temperatures were selected based on the thermal decomposition behavior of zinc acetate and nickel acetate, ensuring proper film formation without undesired by-products or incomplete reactions. The solution was applied by generating an aerosol using an OPH1RAC004D airbrush equipped with a nozzle of diameter d = 0.3 mm. The air pressure for the airbrush was supplied using an AS186 oil-free piston compressor. ZnO was synthesized usingaqueous solutions of the corresponding metal salts. Zinc acetate [$Zn(CH_3COO)_2 2H_2O$] was used as the precursor for the synthesis of the ZnO film. The concentration of the metal salts in the solution was 0.25 M. The synthesis of nickel oxide was carried out using an aqueous solution of nickel acetate [$Ni(CH_3COO)_2\ 2H_2O$], with a molar concentration of nickel in the solution being 0.1 M. Distilled water was used as a

solvent in a volume of 200 ml. Hydrochloric acid (1 mL) was added to prevent the hydrolysis of nickel acetate in water. The solution was stirred for 30 min. Stirring was performed at room temperature using an magnetic stirrer IKARHbasic2. The parameters for applying NiO were as follows: compressor pressure, 1.5 bar, distance from the aerosol source to the substrate, 80 cm and solution flow rate, 7 ml/min. To maintain the temperature regime during the deposition process, a 4-minute pause was observed every 6 min. After deposition of the NiO film, isothermal annealing was performed at 500°C for 3 h to reduce the resistance through crystallization. ZnO film deposition was carried out at an air pressure of 2 bar at a speed of 8 ml/min. The distance from the sputtering head to the preheated glass target was 85 cm. Multilayer deposition of the ZnO film took place for 1 min with a subsequent break of 30 s to restore the substrate temperature. Thus, a total of 14 layers were obtained. To fabricate the n-ZnO–p-NiO structure, n-ZnO films were first grown on borosilicate glass substrates under the aforementioned conditions and subjected to thermal treatment. Subsequently, p-NiO films were grown on half of the surface of the grown n-ZnO film and the prepared samples underwent thermal treatment. X-ray diffraction measurements were performed in the Bragg-Brentano beam geometry in the range of $2\theta_B$ = from 20° to 80° at a scanning rate of 2°/min. The electrophysical properties of the fabricated n-ZnO-p-NiO structures were studied using the van der Pauw method at room temperature and the conductivity of the solid solutions was determined using a thermoprobe as well as by the sign of the Hall constant.

3. Results and Discussion

X-ray structural studies of the grown metal oxide films ZnO, NiO and the structure of n-ZnO-p-NiO were carried out using a third-generation Empyrean Malvern X-ray diffractometer (Zaynabidinov *et al*., 2024c). Figure 1*a* shows the X-ray diffraction (XRD) patterns of the deposited ZnO films. It can be seen that at low-angle scattering, diffuse reflection with three highly intensive selective structural reflexes is observed, belonging to the crystallographic orientation (100) at a scattering angle of 2θ=31.42° with d/n = 0.2774 nm, (002) at an angle of 2θ = 34.48° with d/n = 0.2581 nm and (101) at a scattering angle of 2θ = 36.34° with d/n = 0.249 nm. Among these observed reflexes, the structural line belonging to the crystallographic direction (002) has the highest intensity (~104imp·c-1) and based on these experimental values, we determined the full width at half maximum (FWHM) of this reflection to be $3.9 \cdot 10^{-3}$ rad, indicating a sufficiently high degree of crystallinity of the grown film. Analysis of the experimental results revealed that the ZnO films exhibited a hexagonal wurtzite structure with lattice constants of a = b = 0.3265 nm and c = 0.5212 nm. This structure belongs to the spatial group C6/mmc, which is characterized by an alternate arrangement of zinc and oxygen atoms in the elementary cell of the crystal lattice. Furthermore, the sizes of the subcrystallites in the undoped ZnO films were determined based on the experimental values of the reflection shape (002) of the X-ray diffraction pattern, which were approximately ~39.5 nm. Additionally, in the X-ray diffraction pattern of the grown films in the range of scattering angles 47.0°÷47.48°, double structural reflections belonging to the crystallographic orientations (111) and (102) are observed, corresponding to the substrate ($SiBO_3$) and ZnO film, respectively[(JCPDS 036-1451)] (Figure 1).

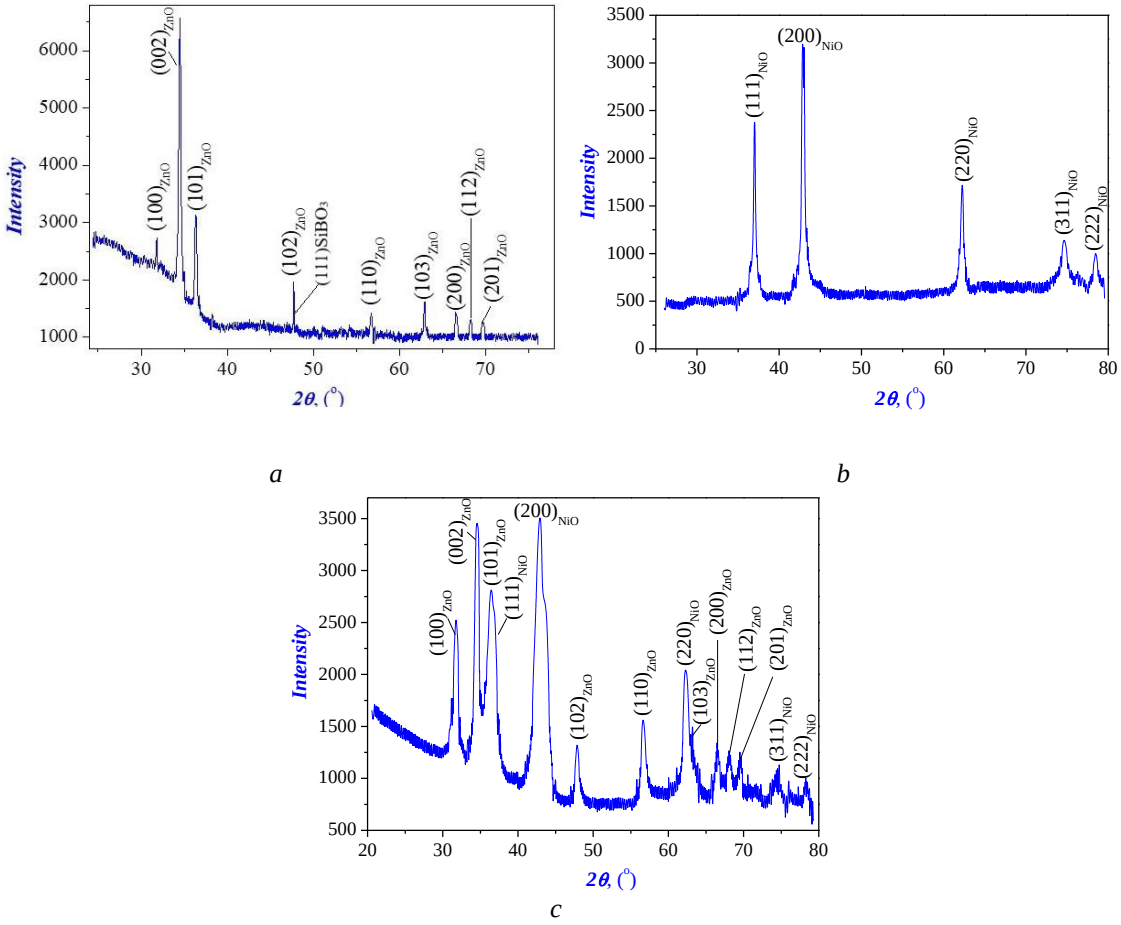

Figure 1. X-ray diffraction pattern of ZnO films (a), NiO film (b) and n-ZnO-p-NiO structure (c)

In addition, the structural lines observed in the X-ray diffraction pattern correspond to crystallographic orientations (110) at an angle of 2θ = 56.67° with d/n = 0.1630 nm, (103) at an angle of 2θ = 62.93° with d/n = 0.1481 nm, (200) at an angle of 2θ = 66.37° with d/n = 0.1398 nm, (112) at an angle of 2θ = 66.52° with d/n = 0.1376 nm and (201) at an angle of 2θ = 69.17° with d/n = 0.1327 nm. This, in turn, indicates that polycrystalline regions with sizes of 12.6 nm, 28.3 nm, 30 nm and 33 nm, as well as nanocrystallites with sizes of 56.8 nm, are self-formed at the boundaries of subcrystallitesin the grown ZnO films near-surface layers.

Figure 1*b* shows X-ray diffraction patterns of the deposited NiO films, which significantly differ from the X-ray diffraction pattern of pure ZnO films. It is evident that the diffuse reflection observed in low-angle scattering is absent. Additionally, at scattering angles of 2θ = 36.9° with d/n = 0.2434 nm, 2θ = 42.89° with d/n = 0.2108 nm and 2θ = 62.28° with d/n = 0.1491 nm, the X-ray diffraction patterns of the NiO film exhibit more intense diffraction peaks from the (111), (200) and (220) crystallographic planes, respectively (JCPDS 004-0835).

Based on the experimental results of these reflections, the lattice parameter of the deposited NiO films was determined to be $a_{f.NiO}$ = 0.4178 nm. This indicates that the elementary cell of the film belongs to the cubic spatial group Fm3m, with a lattice parameter of 0.4178 nm. Furthermore, from the experimental values of these structural lines, it was established that the main blocks of the film were 22.3 nm, 29.3 nm and 16.9 nm, respectively.

At large specific angles, an increase in the level of the inelastic background is observed in the X-ray diffraction patterns of the film (Weerathunga *et al*., 2022). This, in turn, indicates a high number of structural microdistortions within the volume of the film compared to its surface. Typically, second- and third-order structural reflections are observed at large angles in the X-ray pattern. This indicates that the arrangement of atoms corresponds to a plane within the elementary cell. Therefore, an abnormal increase in the background level of the second- or third-order structural reflections suggests the formation of microstresses in the atomic bonds within the elementary cell. Another confirmation of our hypothesis is that the structural lines belong to the (311) and (222) crystallographic orientations at scattering angles θ = 74.6° with d/n = 0.1271 nm and 2θ = 78.6° with d/n = 0.1217 nm, respectively, in the X-ray diffraction patterns of the film. The broadening and low intensity of this structural line indicate the formation of clusters with sizes of 5 nm and 7 nm, respectively, within the volume of the grown film. This suggests the presence of amorphous regions without long-range order within the film volume. The authors of (Utamuradova *et al*., 2024) determined that the formation of small-scale clusters in films leads to short-range ordering of the atoms, revealing their amorphous properties.

Figure 1*c* shows the X-ray diffraction pattern of the n-ZnO–p-NiO structure. In contrast to the metal oxide films n-ZnO and p-NiO, the X-ray diffraction pattern of the n-ZnO-p-NiO structure exhibited a slight change in the structural reflexes belonging to both components (the intensities decreased and shifted towards low-angle scattering). This, in turn, indicates a mismatch between the structural parameters of the n-ZnO and p-NiO metal oxide films. Such structural mismatches lead to the appearance of various microstrains in the crystal lattice of the transition layer that is at the interfaces of the deposited films. The fact that the inelastic background level of the XRD pattern of the n-ZnO-p-NiO structure is 40-45% higher than the inelastic background level of the XRD patterns of the metal oxide films n-ZnO and p-NiO confirms our aforementioned opinions. Furthermore, a change in the elastic background level of the XRD pattern of the n-ZnO-p-NiO structure was also observed in the scattering angle range of 60-80 degrees, indicating an approximation to a diffraction form. This suggests a close order of atomic bonding between the metal oxide films of n-ZnO and p-NiO in the regions near the transition layer (Sarang *et al.*, 2019). Such close-ordered bonds confirmed the formation of small clusters and voids within the films.

The optical properties of the grown films were studied using a CaryEclipse fluorescence spectrophotometer in the spectral range–190-1100 nm. The optical transmittance spectra (red curves) of the ZnO films are shown in Figure 2. It can be observed that the ZnO film exhibited high transmittance, starting at 378 nm. Metal oxide films of ZnO, as investigated by Rembeza et al. (2017; 2022), have an optical transmittance of 90% starting from ~360 nm. Since ZnO is a direct bandgap material, the absorption coefficient (α) can be determined using the following relationship (Joshi & Kiani, 2021):

$$\alpha h\nu = A(h\nu - E_g)^{1/2}, \quad (1)$$

where $h\nu$ is the photon energy, A is the absorption proportionality constant calculated based on experimental optical transmittance results (T) and E_g is the bandgap energy. The absorption coefficient (α) can also be calculated from the transmittance coefficient (T) using the following expression (Adachi, 1999):

$$\alpha = \frac{1}{d} ln \frac{1}{T}, \quad (2)$$

where *d* denotes the thickness of the glass substrate. Knowing the values of the absorption coefficient (α), photon energies $(h\nu)$ and proportionality constant (A), the bandgap width of the investigated ZnO film was estimated to be 3.27 eV, confirming that these values closely match those reported in (Aboud *et al.*, 2019). Furthermore, Figure 2 shows the optical transmittance spectra of the grown NiO films (black curve). It can be seen from the figure that the thin film has a high transmittance coefficient, starting from 325 nm. The NiO films also exhibited transmittance spectra ranging from 56% to 68% in the visible and near-infrared regions. The band gap width of the investigated NiO film was estimated to be 3.81 eV using (1). The optical transmittance spectra of ZnO/NiO films are shown in Figure 2 (green curves). It is evident from the figure that the optical transmittance of the ZnO/NiO films decreased sharply to 37% and had a transmittance coefficient starting at 380 nm. In this case, the band gap width of the ZnO/NiO films was 3.26 eV. The optical transmittance of the n-ZnO/p-NiO film decreased owing to the sequential growth of the ZnO and NiO films.

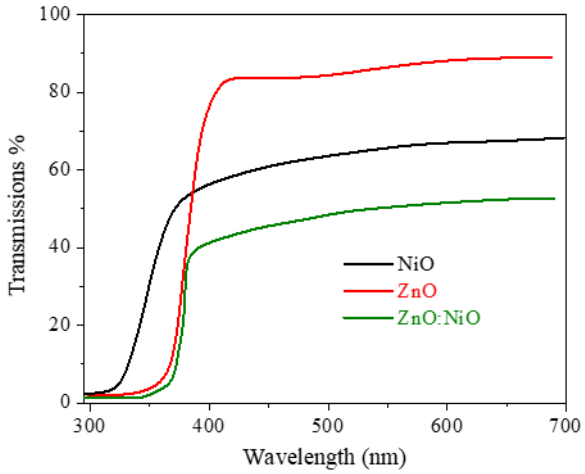

Figure 2. Optical transmittanceof ZnO (red curve), NiO (black curve) and ZnO/NiO (green curve) films

Given that the investigation of the electrophysical properties of n-ZnO-p-NiO structures places special emphasis on the quality of the ohmic contacts, their compositions and application conditions were carefully selected. This implies that carrier injection should not occur at the contact and there should be a linear relationship between the current and voltage under both polarity conditions; the contact must strictly be ohmic (Laya *et al.*, 2022). In our case, this is achieved by creating a region of strong semiconductor doping between the metal and semiconductor. To obtain ohmic contacts in the semiconductor structures of n-ZnO–p-NiO, we used the following materials: Au and Ag.

The quality of the obtained ohmic contacts was initially evaluated using a characterograph, followed by voltage drop measurements and determination of their resistance.

For the hole-type conductivity in p-NiO metal oxide films, contacts with the lowest specific resistance and good linearity were achieved by vacuum deposition of Au and Ag onto the surface of the layers, followed by annealing at 150°C (Guziewicz *et al.*, 2011).

The metal oxide layers predominantly turned out to be of the hole type of conductivity and such samples were mainly used for research, that is, layers with the hole type of conductivity (Patel & Gupta 2022).

The results demonstrate an enhancement in the electrical properties of the n-ZnO and p-NiO films. Specifically, the n-ZnO film exhibited a resistivity of ρ = 16.2 Ω·cm, a carrier concentration of N = 16.7 × 10^{15} cm^{-3} and a carrier mobility of μ = 23.1 $cm^2/V·s$. In comparison, the p-NiO film showed a resistivity of ρ = 0.57 Ω·cm, a carrier concentration of N ≈ 10^{17} cm^{-3} and a carrier mobility of μ ≈ 114 $cm^2/V·s$.

Since the device characteristics of heterodiodes are mainly determined by the mechanisms of current flow through the heterojunction boundaries, the study of volt-ampere and capacitance-voltage characteristics of heterojunction structures and the influence of various external factors on them is one of the current tasks. Therefore, this section presents the results of the research on the volt-ampere and capacitance-voltage characteristics of n-ZnO-p-NiO structures.

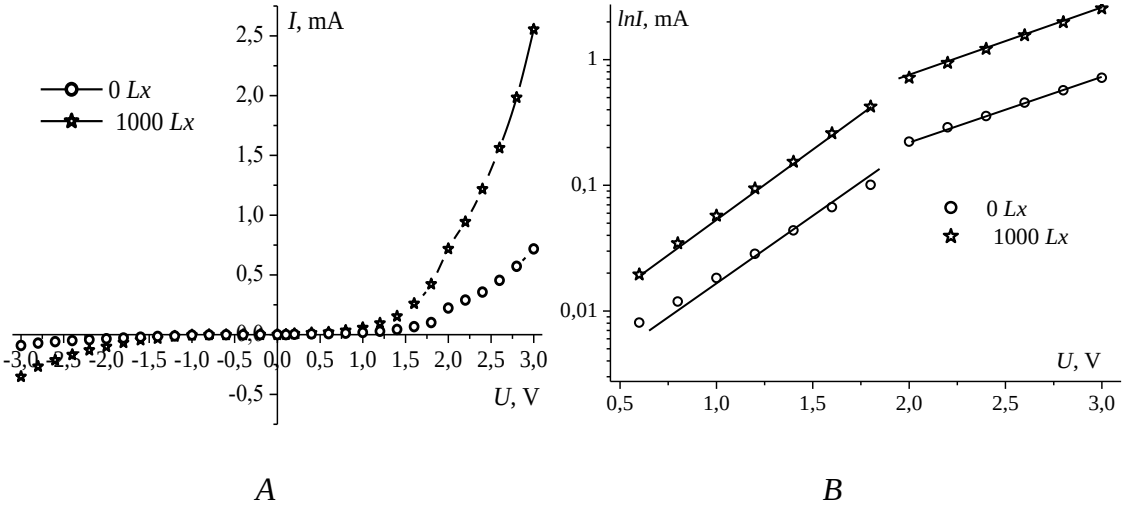

Figure 3. Volt-ampere characteristic of the n-ZnO-p-NiO structure (a) and its conversion to a logarithmic scale (b) under illumination E=0 Lx and E=1000 Lx

The volt-ampere characteristics were measured using a standard method with a probe setup at room temperature. A stabilized power supply (DCPowerSuplyHY3005) and digital multimeter (MASTECH M3900) were used in the ammeter and voltmeter modes. To conduct experiments on the volt-ampere characteristics (VAC), n-ZnO-p-NiO structures were selected. The VAC of n-ZnO-p-NiO structures contained regions where, as in the study (Martyshov *et al.*, 2021), the tunnel-recombination mechanism predominates in current flow through the heterojunction (Figure 3a), meaning that two consecutive exponential regions are observed in the current-voltage dependencies, with shapes not dependent on illumination (Figure 3b).

This voltage-ampere characteristic (VAC) can be approximated using the following formula (Mizginov *et al.*, 2023):

$$I = I_{01}\exp(\alpha_1 V) + I_{02}\exp(\alpha_2 V)\,, \qquad (3)$$

where α_1= 2,5 and α_1 = 1,5 respectively. The rectification coefficient of this structure varies from 10 to 300 depending on the technological conditions.

The reverse branch of the I-V characteristics of these heterojunctions can be described by the following expression (Brus & Maryanchuk, 2014):

$$I_{\text{обр}} = \text{A}V_{\text{обр}}^{m}\,, \tag{4}$$

where m = 8 for voltages up to 1 V and m = 10 for higher voltages.

The formation of a high-resistance layer is likely associated with the intense evaporation of nickel from the melt, which occurs at a relatively high temperature and the diffusion of nickel atoms onto the surface of n-ZnO which was positioned in close proximity to the melt before the deposition process began.

The authors of studies (Lampert & Mark, 1973; Leiderman, 1987) predicted the formation of a high-resistance layer at the transition layer boundary based on the observation of the relationship $I = AV^m$ (where *m* equals 8 to 10) in the reverse direction of the volt-ampere characteristic. Therefore, we assumed the presence of an initial high-resistance layer consisting of Ni and oxygen atoms on the surface of the ZnO film.

There is a possibility that donor impurities in the layer are compensated for by the atoms of nickel that diffuse into it (Sun *et al*., 2011). This hypothesis is supported by the experimental observation that increasing the holding time of the layer in this position resulted in an increase in the thickness of the high-resistance layer. Therefore, the fabricated samples represent a heterostructure of n-ZnO-p-NiO type.

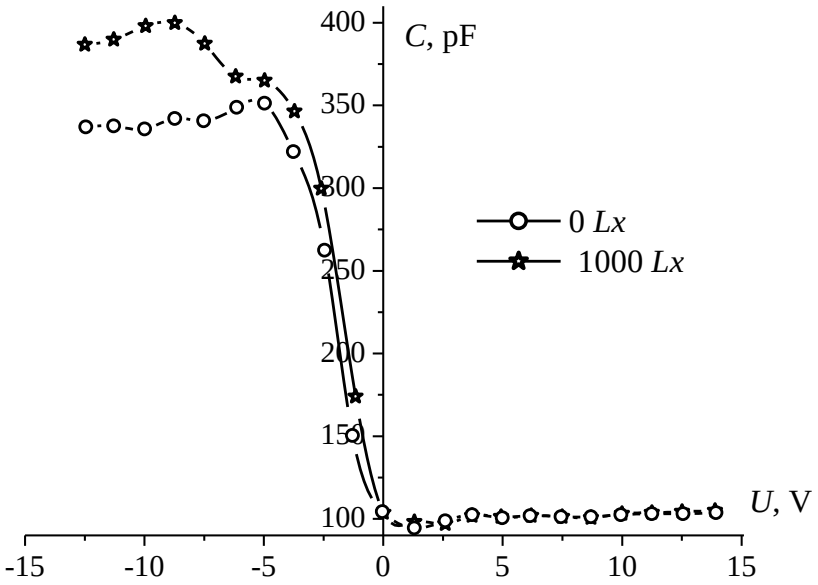

Figure 4. Capacitance-voltage characteristics of the n-ZnO-p-NiO structure under illumination conditions of E=0 Lx and E=1000 Lx

Measurements of the volt-capacitive characteristics of the n-ZnO-p-NiO structure were conducted at a temperature of 300 K and a frequency of 1 MHz using the ES-12 setup. The volt-frequency characteristics were investigated under illumination with E=0 lx and E=1000 lx (Figure 4) (0 lux represents darkness, while 1000 lux represents the threshold under light conditions at which changes in the photoelectric properties of research samples can be detected). The maximum capacitance was observed in the negative voltage region, which corresponded to the p-type conductivity of the NiO films.

Under illumination of E=1000 lx, the capacitance of the heterostructure increases at negative voltages, whereas at positive voltages, the capacitance of the heterostructures remains almost constant and minimal (~110 pF). The voltage-frequency characteristics (VFC) of the heterostructure exhibit steps and peaks along the voltage axis *U*. This behavior in high-frequency VFC indicates the presence of a monoenergetic level of fast surface states at the heterojunction.

4. Conclusion

Based on the experimental research and analysis of the obtained results, the following conclusions can be drawn:

The optimal duration (t = 30 min) and temperature (500°C) for thermal treatment to obtain high-quality ZnO, NiO and ZnO/NiO films were determined.

- it has been established that the surface of the grown ZnO films exhibits a crystallographic orientation (002) and consists of blocks with dimensions of 39.5 nm, possessing a hexagonal crystal lattice with parameters a = b = 0.3265 nm and c = 0.5212 nm, belonging to the space group C6/mmc. Additionally, polycrystalline regions of sizes 12.6 nm, 28.3 nm, 30 nm and 33 nm, as well as nanocrystals with a size of 56.8 nm, self-form both in the bulk and on the surface of the films;

It was determined that the elementary cell of the deposited NiO films belonged to the space group Fm3m, with lattice parameters of 0.4178 nm. The sizes of the main blocks of the NiO films were found to be 22.3 nm, 29.3 nm and 16.9 nm, respectively;

- discovered that the level of inelastic background in the X-ray diffraction pattern of the n-ZnO-p-NiO structure is 40-45% higher than the level of inelastic background in the X-ray diffraction patterns of the n-ZnO and p-NiO metal oxide films, attributed to the formation of small clusters and voids within the films;

- it was found that the grown ZnO and NiO films exhibit high transmittance coefficients ranging from 74% to 92% and from 56% to 68% in the visible and near-infrared regions of the spectrum, respectively. It was determined that the bandgap widths of the ZnO, NiO and ZnO/NiO films are 3.27 eV, 3.81 eV and 3.26 eV, respectively;

The volt-ampere characteristics (VAC) of the n-ZnO-p-NiO structure were investigated under illumination at 0 and 1000 lx. It was shown that in the n-ZnO-p-NiO structures, current conduction was determined by a tunnel-recombination mechanism. The voltage-frequency characteristics (VFC) of the n-ZnO-p-NiO structure revealed that regions with higher specific resistances were formed at the heterojunction.

Funding

The work was carried out using project funds allocated according to the order of the rector of Andijan State University dated February 7, 2024, No. 04-12.

References

Aboud, A.A., Shaban, M. & Revaprasadu, N. (2019). Effect of Cu, Ni and Pb doping on the photo-electrochemical activity of ZnO thin films. *RSC Advances*, *9*(14), 7729-7736. https://doi.org/10.1039/c8ra10599e

Adachi, S. (1999). *Optical Properties of Crystalline and Amorphous Semiconductors: Materials and Fundamental Principles*. New York, Science & Business Media, 147.

Askerov, S.G., Gasanov, M.G., & Abdullayeva, L.K. (2022). The influence of the metal microstructure on the breakdown mechanism of Schottky diodes. *Materials Physics and Chemistry*, *4*(1), 1-6.

Brus, V.V., Maryanchuk, P.D. (2014). Photosensitive Schottky-type heterojunctions prepared by the drawing of graphite films. *Applied Physics Letters*, *104*(17). http://scitation.aip.org/content/aip/journal/apl/1 04/17/10.1063/1.4872467

Dejam, L., Solaymani, S., Kulesza, S., Ghaderi, A., Ţălu, Ş. & Bramowicz, M. (2022). ITO: n-ZnO: p-NiO and ITO: n-ZnO: p-NZO thin films: Study of crystalline structures, surface statistical metrics and optical properties. *Microscopy Research and Technique*, *85*(11), 3674-3693. https://doi.org/10.1002/jemt.24220

Di Mauro, A., Cantarella, M., Nicotra, G., Privitera, V. & Impellizzeri, G. (2016). Low temperature atomic layer deposition of ZnO: Applications in photocatalysis. *Applied Catalysis B: Environmental*, 196, 68-76.

Geleta, T.A., Imae, T. (2021). Nanocomposite photoanodes consisting of p-NiO/n-ZnO heterojunction and carbon quantum dot additive for dye-sensitized solar cells. *ACS Applied Nano Materials*, *4*(1), 236-249. https://doi.org/10.1021/acsanm.0c02547

Guziewicz, M., Grochowski, J., Borysiewicz, M., Kaminska, E., Domagala, J.Z., Rzodkiewicz, W. & Piotrowska, A. (2011). Electrical and optical properties of NiO films deposited by magnetron sputtering. *Optica Applicata*, *41*(2).

Ilin, A.S., Ikim, M.I., Forsh, P.A., Belysheva, T.V., Martyshov, M.N., Kashkarov, P.K. & Trakhtenberg, L.I. (2017). Green light activated hydrogen sensing of nanocrystalline composite ZnO-In_2O_3 films at room temperature. *Scientific Reports*, *7*(1), 12204. https://doi.org/10.1038/s41598-017-12547-5

Jlassi, M., Sta, I., Hajji, M., Haoua, B.B. & Ezzaouia, H. (2014). Effect of annealing atmosphere on the electrical properties of nickel oxide/zinc oxide p-n junction grown by sol-gel technique. *Materials Science in Semiconductor Processing*, 26, 395-403. https://doi.org/10.1016/j.mssp.2014.05.008

Joshi, S., Kiani, A. (2021). Hybrid artificial neural networks and analytical model for prediction of optical constants and bandgap energy of 3D nanonetwork silicon structures. *Opto-Electronic Advances*, *4*(10), 210039-1. https://doi.org/10.29026/oea.2021.210039

Lampert, M., Mark, P. (1973). *Injection Currents in Solids*. Moscow, Mir, 210-225. (In Russian).

Leiderman, A.Yu. (1987). Recombination and relaxation processes in semiconductors with impurity complexes. In *Physics and Materials Science of Semiconductors with Deep Levels*. Moscow, 232. (In Russian).

Mansurov, K.J., Boboev, A.Y. & Urinboyev, J.A. (2024). X-Ray structural and photoelectric properties of SnO_2, ZnO and Zn_2SnO_4 metal oxide films. *East European Journal of Physics*, 2, 336-340.

Martyshov, M.N., Smirnova, V.V., Ilin, A.S. & Forsh, P.A. (2023). Conductivity features of ZnO and NiO nanofiber composites. *Technical Physics Letters*, *49*(2), 35-37.

Martyshov, M.N., Smirnova, V.V., Ilyin, A.S., Platonov, V.B., Forsh, P.A. & Kashkarov, P.K. (2021). Conductivity features of ZnO and NiO nanofiber composites. *Journal of Technical Physics*, *49*(4). https://doi.org/10.21883/PJTF.2023.04.54521.19305

Mizginov, D., Telminov, O., Yanovich, S., Zhevnenko, D., Meshchaninov, F. & Gornev, E. (2023). Investigation of the temperature dependence of volt-ampere characteristics of a thin-film Si_3N_4 memristor. *Crystals*, *13*(2), 323. https://doi.org/10.3390/cryst13020323

Ohta, H., Hirano, M., Nakahara, K., Maruta, H., Tanabe, T., Kamiya, M. & Hosono, H. (2003). Fabrication and photoresponse of a pn-heterojunction diode composed of transparent oxide semiconductors, p-NiO and n-ZnO. *Applied Physics Letters*, *83*(5), 1029-1031. http://dx.doi.org/10.1063/1.1598624

Patel, V.D., Gupta, D. (2022). Solution-processed metal-oxide based hole transport layers for organic and perovskite solar cell: A review. *Materials Today Communications*, 31, 103664. https://doi.org/10.1016/j.mtcomm.2022.103664

Rembeza, E.S. et al. (2022). Structure, properties and applications of ZnO metal oxide films. *Scientific Bulletin Physical and Mathematical Research. Andijan*, *2*(4), 5-11.

Rembeza, S.I., Rembeza, E.S., Svistova, T.V. & Kosheleva, N.N. (2017). Metal oxide films: Synthesis, properties and application. Monograph. VSU Publishing House, 171.

Sarang Dev, G., Sharma, V., Singh, A., Baghel, V.S., Yanagida, M., Nagatakic, A. & Tripathi, N. Raman spectroscopic study of ZnO/NiO nanocomposites based on spatial correlation model. *RSC Advances*, 9, 26956. https://doi.org/10.1039/c9ra04555d

Sun, F., Shan, C.X., Li, B.H., Zhang, Z.Z., Shen, D.Z., Zhang, Z.Y. & Fan, D. (2011). A reproducible route to p-ZnO films and their application in light-emitting devices. *Optics Letters*, *36*(4), 499-501. https://opg.optica.org/ol/abstract.cfm?URI=ol-36-4-499

Tian, H., Fan, H., Dong, G., Ma, L. & Ma, J. (2016). NiO/ZnO p-n Heterostructures and their Gas Sensing Properties for Reduced Operating Temperature. *RSC Advances, 6*(110), 109091-109098. https://doi.org/10.1039/C6RA19520B

Utamuradova, Sh.B., Daliev, Sh.Kh., Bokiyev, B.R. & Zarifbaev, J.Sh. (2024). X-ray spectroscopy of silicon doped with germanium atoms. *Advanced Physical Research, 6*(3), 211-218. https://doi.org/10.62476/apr63211

Wan, J., Xu, Y., Ozdemir, B., Xu, L., Sushkov, A B., Yang, Z. & Hu, L. (2017). Tunable broadband nanocarbon transparent conductor by electrochemical intercalation. *ACS Nano, 11*(1), 788-796. https://doi.org/10.1021/acsnano.6b07191.PMID28033469

Weerathunga, H., Tang, C., Brock, A.J., Sarina, S., Wang, T., Liu, Q. & Waclawik, E.R. (2022). Nanostructure shape-effects in ZnO heterogeneous photocatalysis. *Journal of Colloid and Interface Science*, 606, 588-599.

Xi, Y.Y., Hsu, Y.F., Djurišić, A.B., Ng, A.M.C., Chan, W.K., Tam, H.L. & Cheah, K.W. (2008). NiO⁄ ZnO light emitting diodes by solution-based growth. *Applied Physics Letters*, *92*(11). https://doi.org/10.1063/1.2898505

Xia, Q., Zhao, H., Teng, Y., Du, Z., Wang, J. & Zhang, T. (2015). Synthesis of NiO/Ni nanocomposite anode material for high rate lithium-ion batteries. *Materials Letters*, 142, 67-70. https://doi.org/10.1016/j.matlet.2014.11.142

Xu, M., Li, X., Jin, C., He, Z., Zhang, X. & Zhang, Q. (2020). Novel and dual-mode strain-detecting performance based on a layered NiO/ZnO p-n junction for flexible electronics. *Journal of Materials Chemistry C*, *8*(4), 1466-1474. https://doi.org/10.1039/C9TC05675K

Zainabidinov, S.S., Boboev, A.Y. & Yunusaliyev, N.Y. (2024c). Effect of γ-irradiation on structure and electrophysical properties of S-doped ZnO films. *East European Journal of Physics*, (2), 321-326. https://doi.org/10.26565/2312-4334-2024-2-37

Zainabidinov, S.S., Yulchiev, S.K., Boboev, A.Y., Gulomov, B.D. & Yunusaliyev, N.Y. (2024a). The structural properties of al-doped ZnO films. *East European Journal of Physics*, 3, 282-286. https://doi.org/10.26565/2312-4334-2024-3-28

Zainabidinov, S.Z., Boboev, A.Y., Makhmudov, K.A. & Abduazimov, V.A. (2021a). Photoelectric properties of n-ZnO/p-Si heterostructures. *Applied Solar Energy*, *57*(6), 475-479. https://doi.org/10.3103/S0003701X21060177

Zaynabidinov, S.Z., Yuldashev, S.U., Boboev, A.Y. & Yunusaliyev, N.Y. (2024b). X-ray diffraction and electron microscopic studies of the ZnO<S> metal oxide films obtained by the ultrasonic spray pyrolysis method. *Herald of the Bauman Moscow State Technical University, Series Natural Sciences*, *112*(1), 78-92. https://doi.org/10.18698/1812-3368-2024-1-78-92